Published in final edited form as:
Cancer Res. 2009 April 1; 69(7): 3213–3220. doi:10.1158/0008-5472.CAN-08-4223.

Heterozygosity for *Hypoxia Inducible Factor 1α* decreases the incidence of thymic lymphomas in a p53 mutant mouse model

Jessica A. Bertout[1,2,*], **Shetal A. Patel**[1,3,*], **Benjamin H. Fryer**[1], **Amy C. Durham**[2], **Kelly L. Covello**[1], **Kenneth P. Olive**[1], **Michael H. Goldschmidt**[2], and **M. Celeste Simon**[1,3,4]

[1] Abramson Family Cancer Research Institute, University of Pennsylvania, Philadelphia, PA 19104, USA

[2] School of Veterinary Medicine, University of Pennsylvania, Philadelphia, PA 19104, USA

[3] School of Medicine, University of Pennsylvania, Philadelphia, PA 19104, USA

[4] Howard Hughes Medical Institute, University of Pennsylvania, Philadelphia, PA 19104, USA

Abstract

Hypoxia Inducible Factors (HIFs) are critical mediators of the cellular response to decreased oxygen tension and are overexpressed in a number of tumors. While HIF1α and HIF2α share a high degree of sequence homology, recent work has shown that the two α subunits can have contrasting and tissue-specific effects on tumor growth. To directly compare the role of each HIFα subunit in spontaneous tumorigenesis, we bred a mouse model of expanded HIF2α expression and *Hif1α*$^{+/-}$ mice to homozygotes for the R270H mutation in *p53*. Here we report that *p53*$^{R270H/R270H}$ mice, which have not been previously described, develop a unique tumor spectrum relative to *p53*$^{R270H/-}$ mice, including a high incidence of thymic lymphomas. Heterozygosity for *Hif1α* significantly reduced the incidence of thymic lymphomas observed in this model. Moreover, reduced *Hif1α* levels correlated with decreased stabilization of activated Notch1 and expression of the Notch target genes, *Dtx1* and *Nrarp*. These observations uncover a novel role for HIF1α in Notch pathway activation during T-cell lymphomagenesis.

Keywords

HIF1α; HIF2α; p53; Notch; thymic lymphoma

Introduction

Hypoxia, or decreased oxygen (O_2) availability, is a common characteristic of solid tumors. Cells have developed a number of adaptive responses to O_2 deprivation that are largely mediated by the Hypoxia Inducible Factors (HIFs). HIFs function as αβ heterodimeric transcription factors that regulate over 150 genes involved in metabolism, cell cycle regulation, erythropoiesis, cell survival, and angiogenesis (1,2). The β subunit is constitutively expressed, while the stability of the three α subunits is regulated by O_2 availability. Two HIFα subunits, HIF1α and HIF2α, have drawn considerable interest since their discovery. HIF1α and HIF2α share a high degree of sequence homology but display distinct expression patterns in the adult organism. HIF1α is expressed ubiquitously in the adult, while HIF2α expression is restricted

Corresponding author: M. Celeste Simon, Howard Hughes Medical Institute, Abramson Family Cancer Research Institute, University of Pennsylvania School of Medicine, BRB II/III, Room 456, 421 Curie Boulevard, Philadelphia, PA 19104, Telephone: (215) 746-5532, Fax: (215) 746-5511, E-mail: E-mail: celeste2@mail.med.upenn.edu.
*J.A.B and S.A.P contributed equally to this work.

to the endothelium, kidney, heart, and lung (3–5). In addition, the two subunits have both shared (such as *Vegf*) and unique transcriptional targets. For example, HIF1α exclusively regulates glycolytic enzymes, whereas HIF2α preferentially regulates genes involved in differentiation (*Oct4*) or proliferation (*Epo, Tgf-α*) (6–8).

The observation that HIF1α and HIF2α are highly expressed in a number of human tumors fueled early studies to evaluate the role of each subunit in tumor initiation and progression. Previous attempts to explore the role of HIFs in tumorigenesis utilized subcutaneous models in immunocompromised mice. When injected into mice, transformed $Hif1\alpha^{-/-}$ mouse embryonic fibroblasts grow more slowly and form less vascularized tumors than wild-type fibroblasts, suggesting a role for HIF1α in both tumor growth and angiogenesis (9). In contrast, HIF2α appears to promote the growth of human neuroblastoma and renal clear cell carcinoma tumors in nude mice, whereas HIF1α does not (10–14). Furthermore, HIF2α actually inhibits tumor growth and promotes apoptosis in rat gliomas (15). These studies suggest that the two HIFα subunits have distinct effects on tumorigenesis. They also indicate that either the HIFs have tissue specific functions or that xenografts do not accurately replicate the microenvironment for tumor formation *in vivo*. Introduction of established tumor cell lines subcutaneously in nude mice assesses the capacity of these cells to proliferate and stimulate angiogenesis, but does not evaluate tumor initiation, progression, and metastasis, or the effects of the local microenvironment on tumor growth. A recent study by Liao et al. in a mouse breast cancer model demonstrated that HIF1α is not necessary for tumor initiation, but HIF1α loss results in increased tumor latency and decreased proliferation, angiogenesis, and metastatic potential (16). Since HIFα effects are likely to be tissue- and tumor stage-specific, studies in spontaneous tumor models will be critical to determine the role of each HIFα subunit in cancer.

To this end, we employed our previously described “knock-in” mouse model in which the HIF2α coding sequence is under the control of the *Hif1α* locus ($Hif1\alpha^{KI/+}$), thereby broadening HIF2α expression to all tissues (6,17). In fact, HIF2α has been detected in tumors derived from tissues in which it is not normally expressed (18). This genetic manipulation not only allows us to compare the effect of each subunit directly, as they are expressed in the same tissues, but also avoids non-specific effects from dramatic overexpression encountered in some transgenic models. Homozygous $Hif1\alpha^{KI/KI}$ embryonic stem cells generate more proliferative and vascularized teratomas than their wild-type counterparts, further supporting a role for HIF2α in promoting tumor growth (17). Unfortunately, $Hif1\alpha^{KI/KI}$ mice die before embryonic day 8.5, precluding their use in a tumor study, but heterozygotes are viable (6). Since adult $Hif1\alpha^{KI/+}$ animals do not develop tumors spontaneously (M.C. Simon, unpublished), we induced tumor formation by crossing them to mice bearing an arginine to histidine mutation in codon 270 of p53 ($p53^{R270H}$) (19). The equivalent human mutation (R273H) is commonly detected in patients with Li-Fraumeni syndrome, where patients develop a wide range of tumor types at a young age (19). In contrast to null p53 mutations, R270H mutants develop carcinomas in a number of tissues, suggesting that mutant p53 possesses gain-of-function effects in a tissue-specific manner (20–22). To further accelerate tumorigenesis, we generated $p53^{R270H/R270H}$ (referred to as $p53^{H/H}$) mice, which have not been previously characterized. To determine whether HIF2α could promote tumorigenesis in certain tissues, we evaluated three cohorts with varying HIFα expression for tumor spectrum and onset (Figure 1A). Furthermore, as $Hif1\alpha^{KI/+}$ mice lack one allele of *Hif1α*, we crossed $Hif1\alpha^{+/-}$ mice to p53 mutants as a control for *Hif1α* heterozygosity. This cohort allowed us to further evaluate the role of HIF1α in tumorigenesis.

We report here that $p53^{H/H}$ mice developed a unique tumor spectrum relative to $p53^{H/-}$ animals. A large fraction of $p53^{H/H}$ mice developed thymic lymphomas in a $Hif1\alpha^{+/+}$ background. Interestingly, while expanded HIF2α expression did not impact tumor spectrum or latency, heterozygosity for *Hif1α* (both $Hif1\alpha^{+/-}p53^{H/H}$ and $Hif1\alpha^{KI/+}p53^{H/H}$) significantly reduced the

incidence and increased the age at onset for thymic lymphomas in these mice. Expression profiling of tumors in both *Hif1α* $^{+/-}$*p53*$^{H/H}$ and *Hif1α*$^{KI/+}$*p53*$^{H/H}$ mice revealed reduced Notch activity in tumors heterozygous for *Hif1α*, providing the first demonstration of an interaction between HIF1α and Notch during tumorigenesis.

Materials and Methods

Aging Study

Cohorts were produced by mating *p53*$^{H/+}$ mice to *p53*$^{H/+}$ or *p53*$^{+/-}$ mice. Since the *p53*$^{H/+}$ mice were enriched for $129S_4$/SvJae (19), the *p53*$^{-/-}$ allele was in a mixed C57BL/6-129/Sv background (23), and *Hif1α*$^{+/-}$ and *Hif1α*$^{KI/+}$ mice were 129SvEvTac enriched (6), all mice were of a similarly mixed background. Mice were evaluated daily for signs of morbidity or tumor growth. Distressed mice were euthanized by CO_2 asphyxiation and dissected. All soft tissues were fixed in 4% paraformaldehyde and processed as previously described (19). Tumors were then identified by veterinary pathologists (A.C.D. and M.H.G.).

Immunohistochemistry (IHC)/Immunoblotting

IHC was performed following manufacturer's guidelines and developed using diaminobenzidine (DAB, Vector Labs, Burlingame, CA). Primary antibodies used in this study are listed in the supplement. TUNEL staining was performed using the ApopTag Peroxidase In Situ Apoptosis Detection Kit (Millipore) as per manufacturer's instructions. Positive-staining cells were counted in 8–9 fields per tumor using ImageJ (NIH). Standard techniques were employed for immunoblotting.

RNA extraction and QRT-PCR

Tissues were stored in RNALater (Qiagen). For RNA extraction, tissues were homogenized in Trizol (Invitrogen) and purified using Qiagen RNeasy columns. cDNA synthesis was performed as described previously (24). Taqman primer/probe sets were purchased from Applied Biosystems (Foster City, CA). Microarray analysis was performed at the University of Pennsylvania Microarray Core using the Affymetrix MOE430Av2 array. Raw data for expression profiling are available through the NCBI Gene Expression Omnibus (GEO) with the accession number GSE14336.

Sequencing

The PEST domain of *Notch1* was amplified for sequencing from cDNA using the following primers: 5′-TACCAGGGCCTGCCCAACAC-3′, 5′-GCCTCTGGAATGTGGGTGAT-3′, and 5′-AAGGACCTCAAGGCACGGAG-3′ 5′-GAGGTGTGGCTGTGATGGTG-3′ (25).

Results

Generation of tumor prone mice with expanded expression of HIF2α

To assess the effect of HIF2α on spontaneous tumorigenesis *in vivo*, we crossed *Hif2α* knock-in (*Hif1α*$^{KI/+}$) mice (17) with *p53*$^{H/+}$ animals (19) which are prone to spontaneous tumor formation. As a control for loss of one *Hif1α* allele, we crossed *Hif1α*$^{+/-}$ mice to the same *p53* mutant strain. To generate mice homozygous for the R270H mutation and either wild-type for *Hif1α* (*Hif1α*$^{+/+}$) (n=23), heterozygous for *Hif1α* (*Hif1α*$^{+/-}$) (n=20), or carrying an additional *Hif2α* allele (*Hif1α*$^{KI/+}$) (n=24), we intercrossed heterozygotes for the R270H mutation from each *Hif1α* genotype (Figure 1A). The *Hif1α*$^{KI/+}$ animals were generated in the 129SvEvTac background; therefore, *Hif1α*$^{+/-}$ mice were backcrossed into the 129SvEvTac strain to control for strain differences (6). Successful generation of each cohort was verified by PCR on tail DNA within the first weeks after birth (Figure 1B) and confirmed by repeating

all four PCRs on tail DNA after animal sacrifice (Embark Scientific). To quantify HIF2α expression in normal $Hif1\alpha^{KI/+}$ tissues, QRT-PCR for HIF1α and HIF2α was performed on duodenum and skeletal muscle samples taken from $Hif1\alpha^{+/+}$, $Hif1\alpha^{+/-}$, and $Hif1\alpha^{KI/+}$ mice on a wild-type *p53* background (Figure 1C). As expected, *Hif2α* mRNA levels were increased in normal tissues. Given that our mouse model is one of expanded HIF2α expression and not HIF2α overexpression, these changes (~2 fold) were in the expected range and were similar to levels measured in $Hif1\alpha^{KI/+}$ embryos (6).

Dosage of the $p53^{R270H}$ mutation affects tumor spectrum

Upon dissection, each mouse organ was fixed and prepared for histological analysis, which was conducted by a board-certified veterinary pathologist (A.C.D.). Since the tumor spectrum in mice homozygous for the R270H mutation had not been previously examined, we compared tumor incidence in $p53^{H/H}$ (n=23) mice with $p53^{H/-}$ (n=19) animals in a $Hif1\alpha^{+/+}$ background. Interestingly, $p53^{H/H}$ mice developed substantially more thymic lymphomas (p=0.0015) and tended to present with these tumors at an earlier age than mice in the $p53^{H/-}$ cohort, although the age difference was not statistically significant (Figure 2A–B). Instead, $p53^{H/-}$ mice developed sarcomas (p=0.03), brain tumors and teratomas. Why carcinomas (as described by Olive et al. (19)) were not observed in our $p53^{H/-}$ cohort is unclear, but may be due to subtle changes in growth conditions provided by different animal barrier facilities. Gross and histological findings are provided in Supplemental Figures 3 and 6. The incidence of thymic lymphomas in the $p53^{H/-}$ cohort was consistent with published studies (19). Our $p53^{H/H}$ mice were generated in the $129S_4$/SvJae background (19), a strain less susceptible to lymphomas than C57BL/6 (26). By contrast, the $p53^{-/-}$ mice were of a mixed C57BL/6-129/Sv background (23), which should increase their tendency to develop thymic lymphomas (see Materials and Methods). Thus, the higher incidence of lymphomas in $p53^{H/H}$ mice is likely to be a specific effect of the mutant allele.

As noted previously in $p53^{H/+}$ mice (19), we observed the accumulation of mutant p53 protein by immunohistochemistry on tumor sections obtained from $p53^{H/-}$ and $p53^{H/H}$ animals (Figure 2C). The dramatic increase in thymic lymphoma incidence in $p53^{H/H}$ mice indicates that gain-of-function effects of mutant p53 protein may uniquely or more potently impact thymocytes. Both the increase in number and decrease in age of onset of thymic lymphomas in the $p53^{H/H}$ cohort further suggest that the R270H is not simply a loss-of-function allele.

Loss of one *Hif1α* allele reduces the incidence of thymic lymphomas detected in $p53^{H/H}$ mice

$Hif1\alpha^{+/+}p53^{H/H}$ mice exhibited an abrupt decrease in survival between 100 and 130 days (Figure 3A). These animals were sacrificed due to obvious signs of respiratory distress and displayed large thymic lymphomas upon dissection. $Hif1\alpha^{KI/+}p53^{H/H}$ mice had a significantly different (p=0.026) Kaplan-Meier survival curve with a more gradual decrease in survival, while $Hif1\alpha^{+/-}$ mice showed an intermediate phenotype. When compared to each other, all three curves differed significantly (p=0.046), with $Hif1\alpha^{+/-}p53^{H/H}$ and $Hif1\alpha^{KI/+}p53^{H/H}$ animals typically dying later than $Hif1\alpha^{+/+}$ $p53^{H/H}$ mice. The $Hif1\alpha^{+/-}p53^{H/H}$ and $Hif1\alpha^{KI/+}p53^{H/H}$ survival curves were not significantly different (p = 0.174).

The age at sacrifice for all tumors combined (Figure 3B) and tumor burden (Figure 3C) were not significantly different between genotypes; however, careful gross and histological analysis of each mouse tissue revealed differences in tumor spectra (Figure 4, Supplemental Figure 1). $Hif1\alpha^{+/+}p53^{H/H}$ mice exhibited ~30% more $CD3^+$ thymic lymphomas (Figure 3D, 4, Supplemental Figures 2A, 3–5) than $Hif1\alpha^{+/-}p53^{H/H}$ or $Hif1\alpha^{KI/+}p53^{H/H}$ animals. Instead, $Hif1\alpha^{+/-}p53^{H/H}$ and $Hif1\alpha^{KI/+}p53^{H/H}$ mice were more likely to develop generalized lymphomas (both $B220^+$ B-cell and $CD3^+$ T-cell) infiltrating lymph nodes and other tissues, carcinomas, or teratomas (Figure 3D, Supplemental Figure 2B). These data are consistent with

the difference in Kaplan-Meier curve slopes and suggest that *Hif1α* haploinsufficiency, rather than expansion of HIF2α expression, reduces the incidence of thymic lymphoma in $p53^{H/H}$ mice, allowing other types of tumors to be detected. Pathological findings are tabulated in Supplemental Figures 3–5, and images of tumor types observed during pathological evaluation of $p53^{H/H}$ mice are provided in Figure 4 and Supplemental Figure 1. While these data were not the expected outcome of our experimental design, they suggested an important role for HIF1α in T-cell malignancy.

Age at presentation with thymic lymphomas is significantly increased in $Hif1\alpha^{+/-}p53^{H/H}$ and $Hif1\alpha^{KI/+}p53^{H/H}$ mice

In addition to decreased incidence of thymic lymphomas in $Hif1\alpha^{+/-}p53^{H/H}$ and $Hif1\alpha^{KI/+}p53^{H/H}$ mice, the age at which these animals presented with tumors was also significantly increased (Figure 5A). This difference in latency could be caused by changes in tumor initiation or tumor growth rates. To determine if changes in proliferation rates contributed to altered onset of thymic lymphoma symptoms, we performed immunohistochemistry for the mitotic marker phospho-histone H3 (Ser10) on tumor sections (Figure 5B). However, no significant change in tumor mitotic index was observed. In contrast, TUNEL staining showed increased levels of apoptosis in both $Hif1\alpha^{+/-}p53^{H/H}$ and $Hif1\alpha^{KI/+}p53^{H/H}$ tumors relative to controls (Figure 5C). Since all tumors were harvested after the mice became symptomatic, it is difficult to determine whether the proliferation and apoptosis rates observed in histological sections directly impact tumor progression. Nevertheless, increased apoptosis in $Hif1\alpha^{+/-}p53^{H/H}$ and $Hif1\alpha^{KI/+}p53^{H/H}$ tumors suggests that HIF1α may be important for thymocyte survival, specifically within the stressful environment of a rapidly growing tumor.

To elucidate the molecular basis for the decreased incidence and increased latency of thymic lymphomas in $Hif1\alpha^{+/-}p53^{H/H}$ and $Hif1\alpha^{KI/+}p53^{H/H}$ mice, we next evaluated changes in gene expression between these tumors. QRT-PCR for *Hif2α* in thymic lymphoma tissue collected at the time of sacrifice indicated that, *Hif2α* expression is increased in $Hif1\alpha^{KI/+}p53^{H/H}$ mice (Figure 5D). *Hif1α* mRNA levels were decreased in tumors from $Hif1\alpha^{+/-}p53^{H/H}$ mice, but were surprisingly even lower in the $Hif1\alpha^{KI/+}p53^{H/H}$ cohort. This suggests cross-regulation between the HIFα subunits and may have contributed to the intermediate phenotype of $Hif1\alpha^{+/-}p53^{H/H}$ mice relative to the $Hif1\alpha^{+/+}p53^{H/H}$ and $Hif1\alpha^{KI/+}p53^{H/H}$ cohorts. HIF2α overexpression has been shown to suppress HIF1α levels in renal clear cell carcinoma (14). To determine if increased HIF2α levels alter the expression of HIFα target genes, we also performed QRT-PCR for *Vegf* and *Tgf-α*, two genes preferentially regulated by HIF2α in renal tumors. Increases in *Vegf* and *Tgf-α* mRNA levels in $Hif1\alpha^{KI/+}p53^{H/H}$ mice suggest that HIF2α activity was elevated in these tumors.

To evaluate global changes in gene expression, we performed microarray analysis of five thymic lymphomas from each cohort. One dramatic difference between $Hif1\alpha^{+/+}p53^{H/H}$ and $Hif1\alpha^{+/-}p53^{H/H}$ and $Hif1\alpha^{KI/+}p53^{H/H}$ tumors was *IL-2 receptor-α* (*CD25*), which exhibited a greater than 30-fold change in expression (Figure 6A). Since CD25 is a developmental marker whose expression is closely correlated with Notch activity during T-cell maturation, we hypothesized that differences in *CD25* levels could correspond to differential Notch pathway activation among $Hif1\alpha^{+/+}p53^{H/H}$, $Hif1\alpha^{+/-}p53^{H/H}$ and $Hif1\alpha^{KI/+}p53^{H/H}$ tumors (Figure 6C). During normal T-cell differentiation, Notch1 expression is high at the β-selection checkpoint, when cells receiving appropriate signals through the T-cell receptor begin to proliferate rapidly (Figure 6C). These early stages of development also correspond to CD25 expression. The Notch pathway is then downregulated, cell division ceases, and T-cells continue to mature (27, 28). Given that Notch1 is important for T-cell commitment and proliferation during β-selection, aberrant Notch1 expression after this stage could promote tumorigenesis. To assess

Notch pathway activation in our study, we used QRT-PCR to measure mRNA levels of *Deltex-1 (Dtx1)* and *Notch-regulated ankyrin repeat protein (Nrarp)*, two Notch transcriptional targets (Figure 6A). Both *Dtx1* and *Nrarp* transcript levels were decreased in $Hif1\alpha^{+/-}p53^{H/H}$ and $Hif1\alpha^{KI/+}p53^{H/H}$ thymic lymphomas relative to $Hif1\alpha^{+/+}p53^{H/H}$ tumors, suggesting decreased Notch activity in these tumors.

Notch mutations are common in mouse T-cell acute lymphoblastic leukemia/lymphoma (T-ALL) and occur in the PEST domain of Notch1, a region important for degradation of activated Notch (27). To determine if *Notch1* was mutated in our study, we sequenced the *Notch1* PEST domain in the thymic lymphomas, but only found mutations in one tumor (n=16, data not shown). However, western blots of tumor lysates demonstrated increased stabilization of cleaved Notch1 in $Hif1\alpha^{+/+}p53^{H/H}$ tumors relative to most $Hif1\alpha^{+/-}p53^{H/H}$ and $Hif1\alpha^{KI/+}p53^{H/H}$ samples (Figure 6B). Furthermore, Notch stabilization directly correlated with *Dtx1* and *Nrarp* expression levels. Since Notch promotes T-cell lymphoma growth, decreased Notch activity in $Hif1\alpha^{+/-}p53^{H/H}$ and $Hif1\alpha^{KI/+}p53^{H/H}$ tumors could contribute to the delayed presentation observed in these cohorts. These results suggest that HIF1α promotes the stability of activated Notch, thereby contributing to thymic lymphoma development (Figure 6D).

An alternate mechanism for Notch stabilization is deletion of the E3 ubiquitin ligase *Fbw7* or upregulation of Notch ligands J*agged 1 (Jag1), Jag2, Delta-like-1 (Dll1), Dll3*, or *Dll4*. However, we did not observe decreases in the expression of *Fbw7* or any Notch ligands in our study (data not shown). Instead, it is probable that HIF1α is acting directly to promote Notch stability. Indeed, Gustafsson et al. recently demonstrated in neural and myogenic precursor cells that HIF1α can bind and stabilize activated Notch, promoting its transcriptional activity (29).

Discussion

Xenograft experiments (9,11,12,15) indicate that the HIFα subunits can have differential effects on tumor growth. To evaluate the relative contribution of each HIFα subunit in a more physiologic model of spontaneous tumorigenesis, we analyzed the effect of varying HIFα levels on tumor latency and spectrum in mice homozygous for the R270H mutation in *p53*. While $p53^{H/-}$ and $p53^{H/+}$ mice were previously characterized by Olive et. al (19), $p53^{H/H}$ homozygotes have not been described. We found that $p53^{H/H}$ mice developed substantially more thymic lymphomas than $p53^{H/-}$ animals. Consistent with our observations in mice carrying the R270H mutation, Terzian et. al describe a very high incidence of lymphomas and sarcomas in $p53^{R172H/R172H}$ mice when compared to heterozygotes for the R172H mutation (30). $p53^{H/H}$ mice also present with thymic lymphomas at a younger age. These observations suggest that, at least in thymocytes, the R270H mutant may actively promote tumorigenesis. One potential mechanism for this effect is the observation that *p53* mutants disrupt DNA damage-response pathways (31). Mutations in other DNA damage-response genes, such as *H2ax* and *53bp1*, have also been shown to accelerate thymic lymphoma formation in a p53-null background, illustrating the importance of this pathway as a tumor suppressive mechanism in T-cells (32,33). Moreover, when activated, mutant p53 has the potential to accumulate to higher levels in $p53^{H/H}$ thymocytes as compared to $p53^{H/-}$ thymocytes. Excess stabilized mutant p53 may then promote lymphomagenesis. Of note, mutant p53, stabilized by deletion of MDM2, accelerates tumorigenesis and promotes metastasis in a dose dependent manner (30). The decreased numbers of brain tumors and sarcomas observed in $p53^{H/H}$ mice was likely to be a consequence of this shift towards increased numbers and earlier incidence of thymic lymphomas. Since mice die quickly from respiratory distress once thymic lymphomas have reached a threshold size, it may preclude their living long enough to succumb to other tumor types. The age at which mice had to be sacrificed for sarcomas is greater than that for thymic

lymphomas (189 v. 117 days; Supplemental Figure 3), suggesting that these tumors have a longer latency period. Because fewer $p53^{H/-}$ mice developed thymic lymphomas, other tumor types could be observed.

Using the $p53^{H/H}$ mouse model, we then asked if expanded HIF2α expression could alter tumor spectrum or growth given that many human tumors express high levels of HIF2α. To our surprise, the *Hif2α* knock-in allele had no effect on any of these parameters. This result suggests either that HIF2α is not important for spontaneous tumorigenesis in the $p53^{H/H}$ mouse model, or that HIF2α expression levels achieved in susceptible tissues were insufficient to promote tumor formation. There are also several important differences between the spontaneous tumors observed in $p53^{H/H}$ mice and xenograft models used in previous studies (6,19). Increased HIF2α-mediated *Tgf-α* expression contributes to the growth of both renal clear cell tumors and ES cell-derived teratomas by activating epidermal growth factor receptor signaling; however, a role for this pathway in thymic lymphomas has not been described. Thus, the pro-growth pathways activated by HIF2α may not play an important role in lymphomagenesis, explaining why the $Hif1\alpha^{KI/+}$ allele did not promote thymic lymphoma formation in $p53^{H/H}$ mice. It should also be noted that homozygous $Hif1\alpha^{KI/KI}$ ES cells were used in previous subcutaneous tumor models, where the dosage of HIF2α achieved was significantly higher (6). Moreover, the incidence of teratomas in $p53^{H/H}$ mice was low (only two were observed), so the impact of increased HIF2α expression on spontaneous teratoma formation cannot be adequately determined. The short latency period and limited spectrum of tumors observed in $p53^{H/H}$ mice may also have precluded the detection of subtle HIF2α-mediated effects. A similar study was therefore conducted in $p53^{H/+}$ mice, which develop a wider spectrum of tumors, but the number of mice examined (n≈20) was not large enough to find significant changes in spectrum and latency.

To further study the role of HIF2α in spontaneous tumorigenesis, a conditional knockout model utilizing global, postnatal *Hif2α* deletion may be more valuable (8). Similarly, conditional *Hif1α* deletion will be important to characterize its role at various stages of tumorigenesis, from initiation to growth and metastasis, as well as tissue-specific effects. These studies should reveal the aggregate impact of each of the *α* subunits on tumor promotion or suppression, clarifying potentially conflicting *in vitro* findings. For instance, while HIF1α acutely inhibits proliferation in response to hypoxia by inhibiting c-Myc activity, it also promotes tumor growth by increasing angiogenesis and reprogramming cell metabolism (1). Inhibition of proliferation is likely to be a transient phenomenon that allows cells to adapt to hypoxic stress, and may not translate to reduced tumor growth *in vivo*. The impact of HIF1α on physiologic levels of c-Myc is also different than its effect on overexpressed, oncogenic c-Myc (34). Indeed, in a c-Myc dependent B-cell lymphoma model, HIF1α promotes tumor growth (35). Another important consideration is the difference between constitutive stabilization of the HIFα subunits, as occurs in VHL-deficient renal carcinomas, and more transient oxygen-regulated accumulation.

In $p53^{H/H}$ mice, loss of one *Hif1α* allele significantly reduced the incidence of thymic lymphomas, thus uncovering an important role for HIF1α in thymic lymphomagenesis *in vivo*. In addition, the age at which these mice presented with thymic lymphomas was significantly increased by *Hif1α* haploinsufficiency, suggesting that tumor onset or tumor growth was delayed by decreasing levels of HIF1α. While thymic lymphomas observed in $Hif1\alpha^{+/-}p53^{H/H}$ and $Hif1\alpha^{KI/+}p53^{H/H}$ mice exhibited similar proliferation rates, increased cell death was noted, indicating that HIF1α is important for the survival of thymocytes during tumor growth. To better understand mechanism(s) whereby HIF1α promotes thymic lymphomagenesis, we conducted an unbiased search for gene expression changes correlated with decreased HIF1α. Microarray analysis on thymic lymphoma mRNA from each genotype uncovered a dramatic decrease in CD25 expression, a marker for Notch pathway activity, in

Hif1α$^{+/-}$*p53*$^{H/H}$ and *Hif1α*$^{KI/+}$*p53*$^{H/H}$ tumors. Furthermore, the expression of Notch target genes *Nrarp* and *Dtx1* was also significantly reduced in these tumors. These transcriptional changes suggested that *Hif1α*$^{+/-}$*p53*$^{H/H}$ and *Hif1α*$^{KI/+}$*p53*$^{H/H}$ tumors had reduced Notch activity relative to wild type controls. While mutations in the PEST domain of Notch1, a common feature of mouse T-cell lymphomas, were not observed in our study, loss of one *Hif1α* allele correlated with decreased stabilization of cleaved Notch1. This indicates that HIF1α may be directly involved in stabilizing cleaved Notch or that heterozygosity for *Hif1α* selects against Notch activation. In either case, it appears that differential Notch activation may explain the changes in tumor onset and frequency observed in *Hif1α*$^{+/-}$*p53*$^{H/H}$ and *Hif1α*$^{KI/+}$*p53*$^{H/H}$ mice, as Notch is a critical factor for T-cell lymphoma growth and survival.

Notch pathway activation contributes significantly to the pathogenesis of acute T-ALL in both mice and humans (27). Mouse models have demonstrated that constitutively activated Notch induces murine T-ALL (36–38), and inhibition of Notch in mouse T-ALL cell lines causes cell death (25,39), suggesting that Notch is critical both for induction of leukemogenesis as well as for leukemic cell survival. In addition, overexpression of activated Notch1 is evident in human TALL, and is frequently due to mutations in *Notch1* that lead to constitutive stabilization (25,27,40). As stated above, activating *Notch1* mutations have been observed in multiple mouse models of T-ALL and commonly occur in the PEST domain (26). While we failed to detect *Notch1* PEST domain mutations in most of our tumors, we did observe significantly increased expression of activated Notch1 and downstream Notch transcriptional targets in *Hif1α*$^{+/+}$*p53*$^{H/H}$ tumors as compared to tumors deficient in *Hif1α*, implicating HIF1α in Notch pathway activation.

HIF1α has previously been proposed to increase the stability of activated Notch1 and to promote Notch target activation in myogenic and neural precursor cells (29). However, a role for HIF1α in Notch-driven tumorigenesis had not been demonstrated. Here, we identify an important and novel role for HIF1α in thymic lymphoma development. Mice with normal HIF1α levels exhibit thymic lymphoma-associated morbidity earlier and at a substantially higher incidence than *Hif1α* heterozygous mice. In addition, the tumors exhibit less cell death and higher levels of activated Notch1 and Notch targets than thymic lymphomas arising in *Hif1α* heterozygous mice, implicating HIF1α in Notch pathway regulation during tumorigenesis. This study is also the first to characterize the phenotype of *p53*$^{H/H}$ mice and, in doing so, provides further support for a gain-of-function effect of the R270H mutation.

Supplementary Material

Refer to Web version on PubMed Central for supplementary material.

Acknowledgments

We are thankful to Brian Keith, Warren Pear, and Mark Chiang for advice. We also thank Phyllis Gimotty and Rachel Hammond for statistical analyses, Hongwei Yu and Davesh Shah for technical support, and John Tobias for microarray analysis. Grant support: Howard Hughes Medical Institute, NIH (grants CA104838, R25 CA101871), Veterinary Scientist Training Grant and R25 CA101871 (J.A.B.), Medical Scientist Training Grant and 2-T32-HD-007516-11 (S.A.P). M.C.S. is an investigator of the Howard Hughes Medical Institute.

References

1. Gordan JD, Simon MC. Hypoxia-inducible factors: central regulators of the tumor phenotype. Curr Opin Genet Dev 2007;17:71–77. [PubMed: 17208433]
2. Wenger RH, Stiehl DP, Camenisch G. Integration of oxygen signaling at the consensus HRE. Sci STKE 2005;2005:re12. [PubMed: 16234508]

3. Jain S, Maltepe E, Lu MM, Simon C, Bradfield CA. Expression of ARNT, ARNT2, HIF1 alpha, HIF2 alpha and Ah receptor mRNAs in the developing mouse. Mech Dev 1998;73:117–123. [PubMed: 9545558]
4. Tian H, McKnight SL, Russell DW. Endothelial PAS domain protein 1 (EPAS1), a transcription factor selectively expressed in endothelial cells. Genes Dev 1997;11:72–82. [PubMed: 9000051]
5. Wiesener MS, Jurgensen JS, Rosenberger C, et al. Widespread hypoxia-inducible expression of HIF-2alpha in distinct cell populations of different organs. Faseb J 2003;17 :271–273. [PubMed: 12490539]
6. Covello KL, Kehler J, Yu H, et al. HIF-2alpha regulates Oct-4: effects of hypoxia on stem cell function, embryonic development, and tumor growth. Genes Dev 2006;20:557–570. [PubMed: 16510872]
7. Hu CJ, Wang LY, Chodosh LA, Keith B, Simon MC. Differential roles of hypoxia-inducible factor 1alpha (HIF-1alpha) and HIF-2alpha in hypoxic gene regulation. Mol Cell Biol 2003;23:9361–9374. [PubMed: 14645546]
8. Gruber M, Hu CJ, Johnson RS, et al. Acute postnatal ablation of Hif-2alpha results in anemia. Proc Natl Acad Sci U S A 2007;104:2301–2306. [PubMed: 17284606]
9. Ryan HE, Poloni M, McNulty W, et al. Hypoxia-inducible factor-1alpha is a positive factor in solid tumor growth. Cancer Res 2000;60:4010–4015. [PubMed: 10945599]
10. Holmquist-Mengelbier L, Fredlund E, Lofstedt T, et al. Recruitment of HIF-1alpha and HIF-2alpha to common target genes is differentially regulated in neuroblastoma: HIF-2alpha promotes an aggressive phenotype. Cancer Cell 2006;10:413–423. [PubMed: 17097563]
11. Kondo K, Kim WY, Lechpammer M, Kaelin WG Jr. Inhibition of HIF2alpha is sufficient to suppress pVHL-defective tumor growth. PLoS Biol 2003;1:E83. [PubMed: 14691554]
12. Kondo K, Klco J, Nakamura E, Lechpammer M, Kaelin WG Jr. Inhibition of HIF is necessary for tumor suppression by the von Hippel-Lindau protein. Cancer Cell 2002;1:237–246. [PubMed: 12086860]
13. Maranchie JK, Vasselli JR, Riss J, et al. The contribution of VHL substrate binding and HIF1-alpha to the phenotype of VHL loss in renal cell carcinoma. Cancer Cell 2002;1 :247–255. [PubMed: 12086861]
14. Raval RR, Lau KW, Tran MG, et al. Contrasting properties of hypoxia-inducible factor 1 (HIF-1) and HIF-2 in von Hippel-Lindau-associated renal cell carcinoma. Mol Cell Biol 2005;25:5675–5686. [PubMed: 15964822]
15. Acker T, Diez-Juan A, Aragones J, et al. Genetic evidence for a tumor suppressor role of HIF-2alpha. Cancer Cell 2005;8:131–141. [PubMed: 16098466]
16. Liao D, Corle C, Seagroves TN, Johnson RS. Hypoxia-inducible factor-1alpha is a key regulator of metastasis in a transgenic model of cancer initiation and progression. Cancer Res 2007;67:563–572. [PubMed: 17234764]
17. Covello KL, Simon MC, Keith B. Targeted replacement of hypoxia-inducible factor-1alpha by a hypoxia-inducible factor-2alpha knock-in allele promotes tumor growth. Cancer Res 2005;65:2277–2286. [PubMed: 15781641]
18. Talks KL, Turley H, Gatter KC, et al. The expression and distribution of the hypoxia-inducible factors HIF-1alpha and HIF-2alpha in normal human tissues, cancers, and tumor-associated macrophages. Am J Pathol 2000;157:411–421. [PubMed: 10934146]
19. Olive KP, Tuveson DA, Ruhe ZC, et al. Mutant p53 gain of function in two mouse models of Li-Fraumeni syndrome. Cell 2004;119:847–860. [PubMed: 15607980]
20. Wijnhoven SW, Speksnijder EN, Liu X, et al. Dominant-negative but not gain-of-function effects of a p53. R270H mutation in mouse epithelium tissue after DNA damage. Cancer Res 2007;67:4648–4656. [PubMed: 17510390]
21. Wijnhoven SW, Zwart E, Speksnijder EN, et al. Mice expressing a mammary gland-specific R270H mutation in the p53 tumor suppressor gene mimic human breast cancer development. Cancer Res 2005;65:8166–8173. [PubMed: 16166291]
22. Jackson EL, Olive KP, Tuveson DA, et al. The differential effects of mutant p53 alleles on advanced murine lung cancer. Cancer Res 2005;65:10280–10288. [PubMed: 16288016]
23. Nacht M, Jacks T. V(D)J recombination is not required for the development of lymphoma in p53-deficient mice. Cell Growth Differ 1998;9:131–138. [PubMed: 9486849]

24. Gordan JD, Bertout JA, Hu CJ, Diehl JA, Simon MC. HIF-2alpha promotes hypoxic cell proliferation by enhancing c-myc transcriptional activity. Cancer Cell 2007;11:335–347. [PubMed: 17418410]
25. O'Neil J, Calvo J, McKenna K, et al. Activating Notch1 mutations in mouse models of T-ALL. Blood 2006;107:781–785. [PubMed: 16166587]
26. Attardi LD, Jacks T. The role of p53 in tumour suppression: lessons from mouse models. Cell Mol Life Sci 1999;55:48–63. [PubMed: 10065151]
27. Aster JC, Pear WS, Blacklow SC. Notch signaling in leukemia. Annu Rev Pathol 2008;3:587–613. [PubMed: 18039126]
28. Sjolund J, Manetopoulos C, Stockhausen MT, Axelson H. The Notch pathway in cancer: differentiation gone awry. Eur J Cancer 2005;41:2620–2629. [PubMed: 16239105]
29. Gustafsson MV, Zheng X, Pereira T, et al. Hypoxia requires notch signaling to maintain the undifferentiated cell state. Dev Cell 2005;9:617–628. [PubMed: 16256737]
30. Terzian T, Suh YA, Iwakuma T, et al. The inherent instability of mutant p53 is alleviated by Mdm2 or p16INK4a loss. Genes Dev 2008;22:1337–1344. [PubMed: 18483220]
31. Song H, Hollstein M, Xu Y. p53 gain-of-function cancer mutants induce genetic instability by inactivating ATM. Nat Cell Biol 2007;9:573–580. [PubMed: 17417627]
32. Bassing CH, Suh H, Ferguson DO, et al. Histone H2AX: a dosage-dependent suppressor of oncogenic translocations and tumors. Cell 2003;114:359–370. [PubMed: 12914700]
33. Ward IM, Difilippantonio S, Minn K, et al. 53BP1 cooperates with p53 and functions as a haploinsufficient tumor suppressor in mice. Mol Cell Biol 2005;25:10079–10086. [PubMed: 16260621]
34. Dang CV, Kim JW, Gao P, Yustein J. The interplay between MYC and HIF in cancer. Nat Rev Cancer 2008;8:51–56. [PubMed: 18046334]
35. Gao P, Zhang H, Dinavahi R, et al. HIF-dependent antitumorigenic effect of antioxidants in vivo. Cancer Cell 2007;12:230–238. [PubMed: 17785204]
36. Pear WS, Aster JC, Scott ML, et al. Exclusive development of T cell neoplasms in mice transplanted with bone marrow expressing activated Notch alleles. J Exp Med 1996;183:2283–2291. [PubMed: 8642337]
37. Aster JC, Xu L, Karnell FG, et al. Essential roles for ankyrin repeat and transactivation domains in induction of T-cell leukemia by notch1. Mol Cell Biol 2000;20 :7505–7515. [PubMed: 11003647]
38. Bellavia D, Campese AF, Alesse E, et al. Constitutive activation of NF-kappaB and T-cell leukemia/lymphoma in Notch3 transgenic mice. Embo J 2000;19:3337–3348. [PubMed: 10880446]
39. Sharma VM, Calvo JA, Draheim KM, et al. Notch1 contributes to mouse T-cell leukemia by directly inducing the expression of c-myc. Mol Cell Biol 2006;26:8022–8031. [PubMed: 16954387]
40. Weng AP, Ferrando AA, Lee W, et al. Activating mutations of NOTCH1 in human T cell acute lymphoblastic leukemia. Science 2004;306:269–271. [PubMed: 15472075]

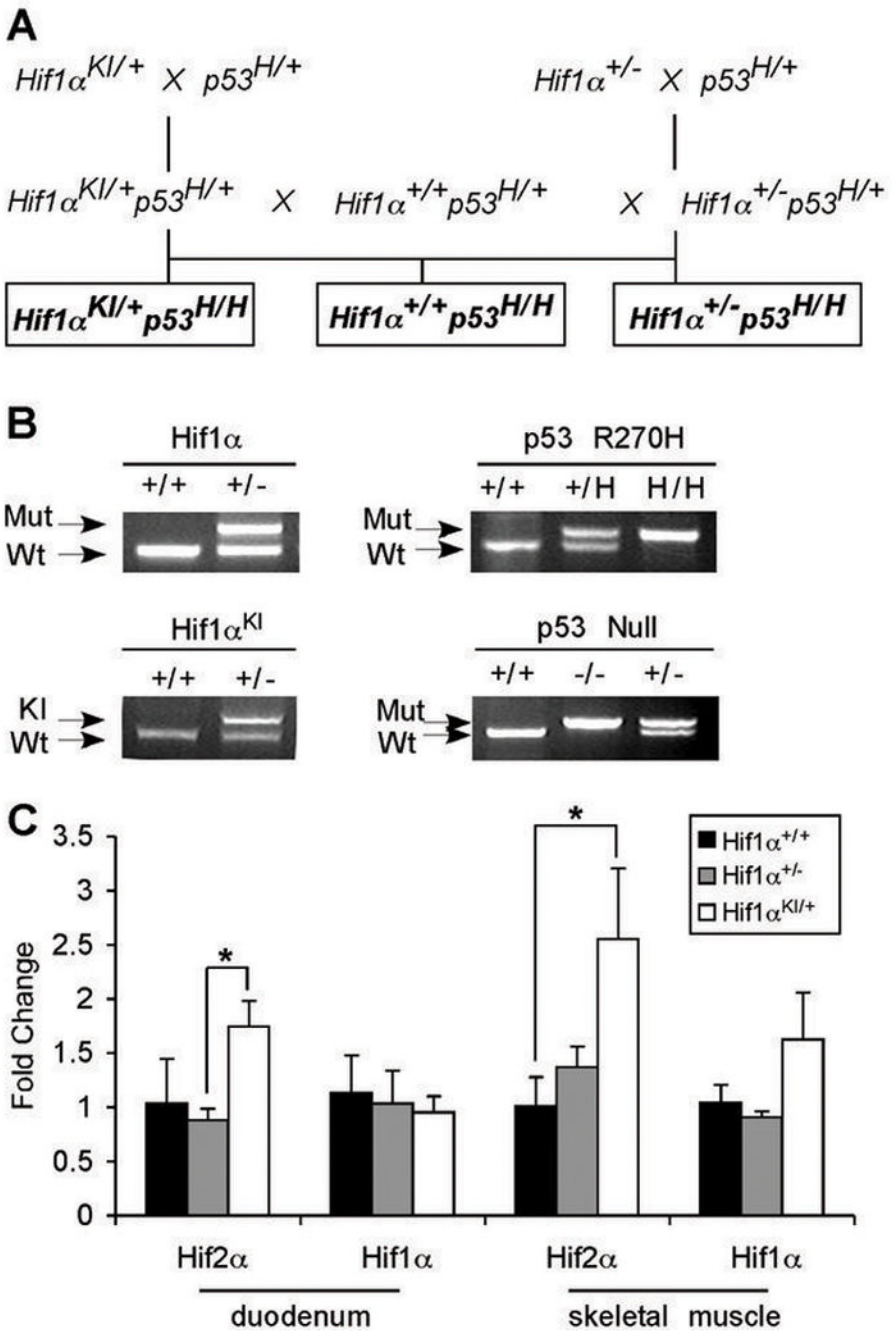

Figure 1. Breeding scheme and characterization of HIF2α expression in adult mouse tissues

A. Breeding scheme to generate *Hif1α*$^{KI/+}$ *p53*$^{H/H}$, *Hif1α*$^{+/-}$*p53*$^{H/H}$, and *Hif1α*$^{+/+}$ *p53*$^{H/H}$ mice. B. Representative genotyping PCR results for each genotype. C. Graph showing *Hif2α* and *Hif1α* mRNA expression in normal duodenum and skeletal muscle of *Hif1α*$^{+/+}$ (black), *Hif1α*$^{+/-}$ (gray), and *Hif1α*$^{KI/+}$(white) mice. *p<0.05

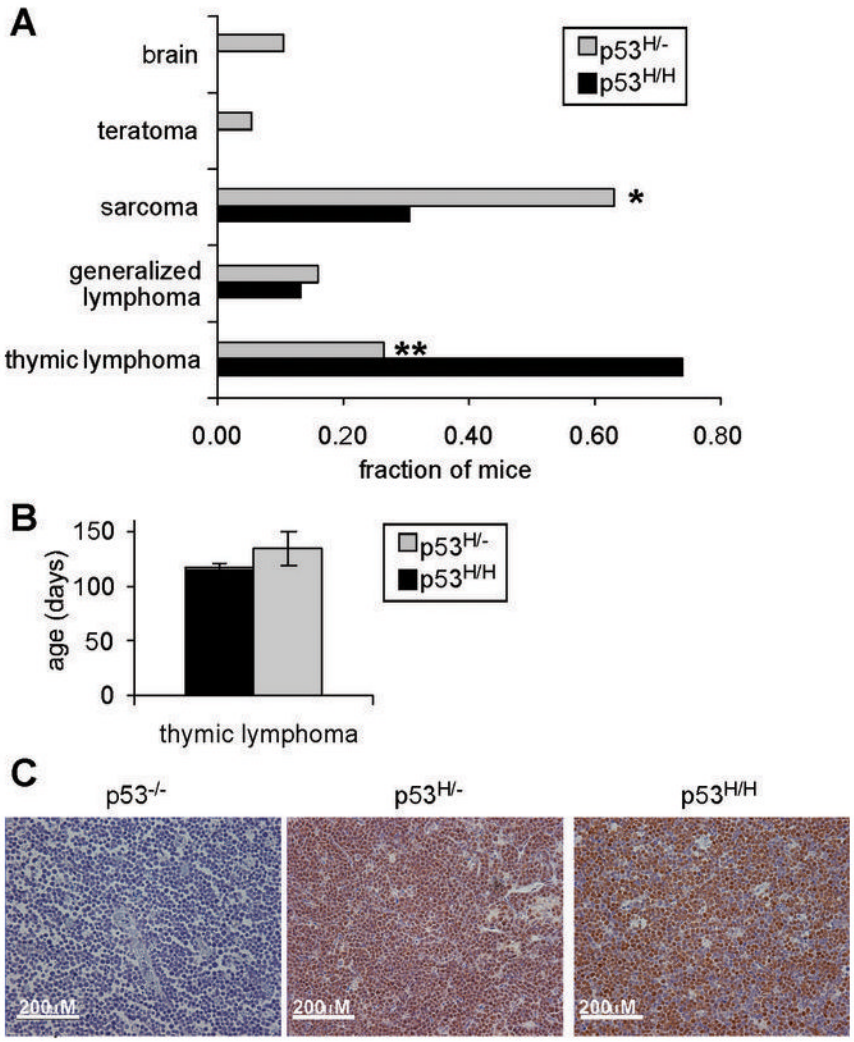

Figure 2. Dosage of *p53*^{R270H} allele influences tumor spectrum

A. Graph comparing tumor types arising in *p53*$^{H/H}$ (n=23, black) and *p53*$^{H/-}$ mice (n=19, gray). * p<0.035; ** p<0.01 B. Age at onset of thymic lymphomas in *p53*$^{H/H}$ and *p53*$^{H/-}$ mice. C. Immunohistochemistry for p53 shows accumulation of mutant protein (brown) in lymphomas from both *p53*$^{H/H}$ and *p53*$^{H/-}$ mice. No p53 protein can be detected in tumors from *p53*$^{-/-}$ mice. Nuclei were counterstained with hematoxylin (blue).

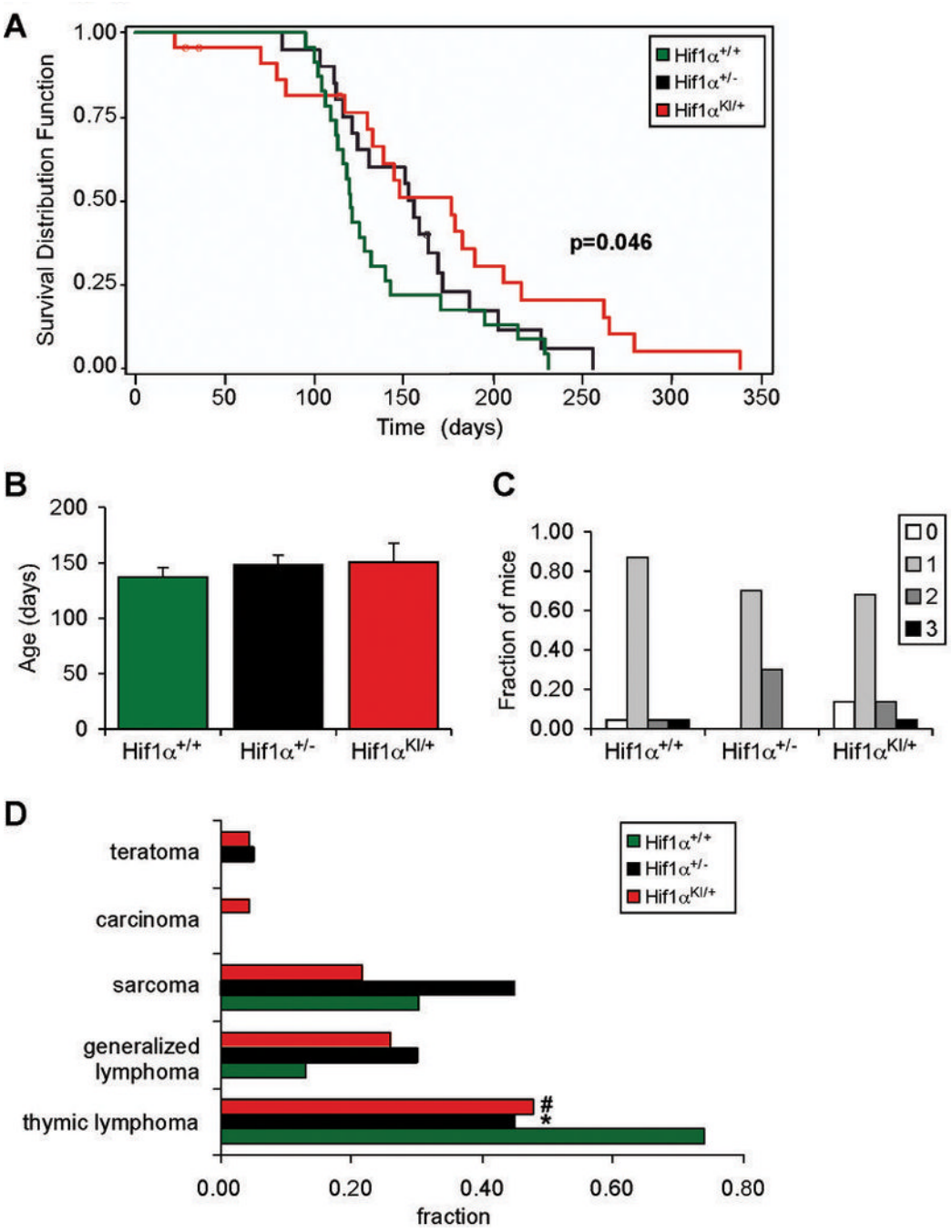

Figure 3. Characterization of survival, tumor spectrum, and tumor burden in *p53$^{H/H}$* mice

A. Kaplan-Meier curve of *Hif1α$^{+/+}$p53$^{H/H}$* (n=23, green), *Hifα1$^{+/-}$p53$^{H/H}$* (n=20, black), and *Hif1α$^{KI/+}$p53$^{H/H}$* (n=24, red) mice. Significance was calculated using a Log-rank test over all three genotypes. When comparing the *Hif1α$^{KI/+}$*p53$^{H/H}$ and *Hif1α$^{+/+}$*p53$^{H/H}$ groups, p=0.024. B. Average age at sacrifice of *Hif1α$^{+/+}$p53$^{H/H}$*, *Hif1α$^{+/-}$p53$^{H/H}$*, and *Hif1α$^{KI/+}$p53$^{H/H}$* mice. C. Tumor burden for *Hif1α$^{+/+}$p53$^{H/H}$*, *Hif1α$^{+/-}$p53$^{H/H}$*, and *Hif1α$^{KI/+}$p53$^{H/H}$* mice. D. Tumor spectrum in *Hif1α$^{+/+}$p53$^{H/H}$*, *Hifα1$^{+/-}$p53$^{H/H}$*, and *Hif1α$^{KI/+}$p53$^{H/H}$* mice. * p = 0.055, # p = 0.073 (student's two-tailed *t* test for pair-wise comparisons).

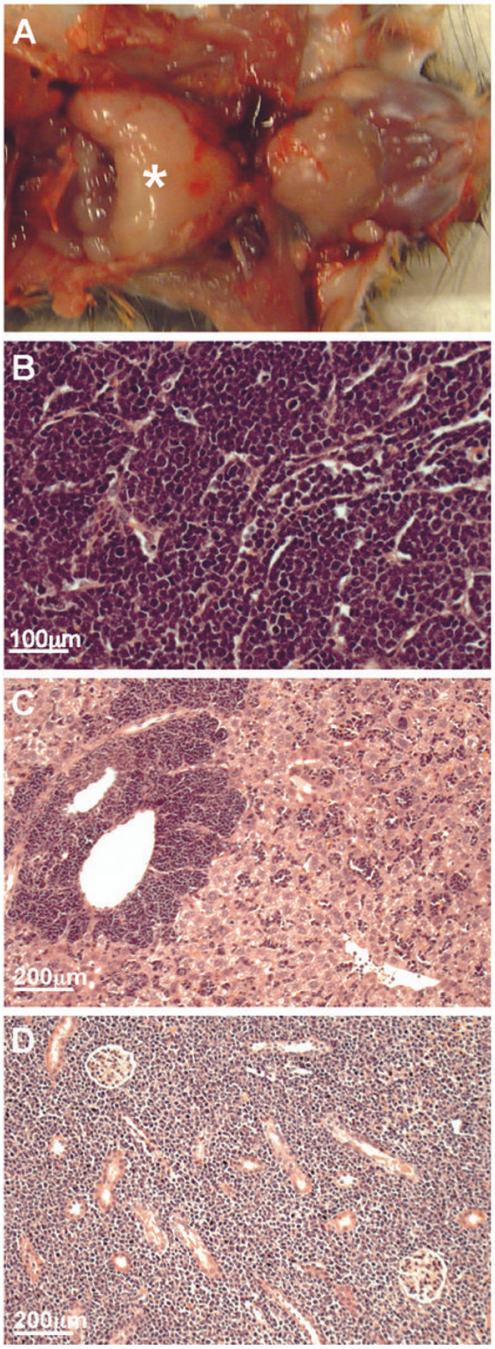

Figure 4. Thymic lymphomas were the predominant tumor type observed in *Hif1α*$^{+/+}$ *p53*$^{H/H}$ mice

A. Gross image of a thymic lymphoma (*) in a dissected mouse. B. Histological section of a thymic lymphoma stained with Hematoxylin and Eosin (H&E). C. H&E of a liver with infiltrating malignant T-cells in a mouse with a thymic lymphoma. D. H&E of a kidney infiltrated with malignant T-cells in a mouse with a thymic lymphoma.

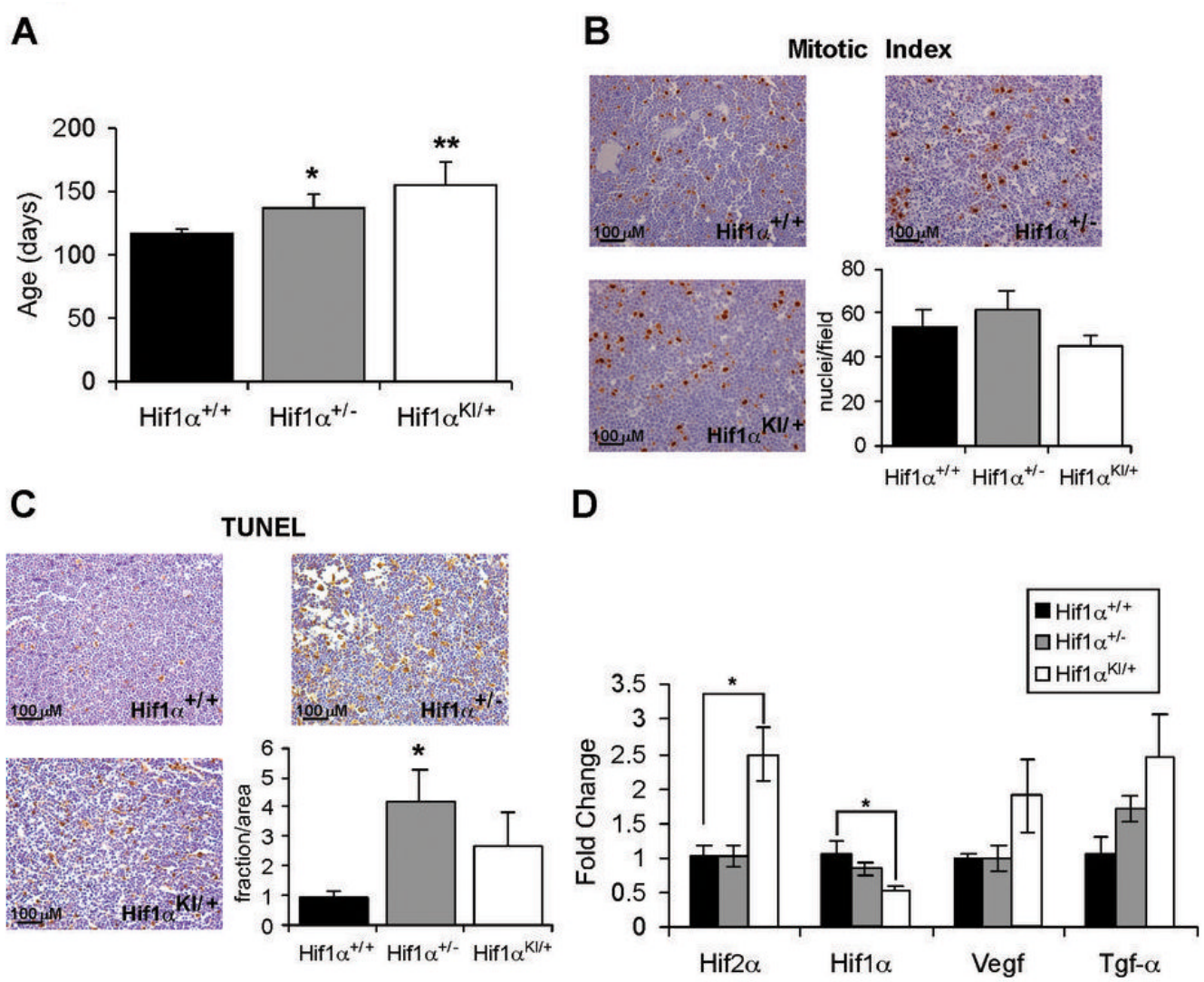

Figure 5. Molecular and phenotypic differences between thymic lymphomas

A. Average age (days) at presentation with thymic lymphoma in *Hif1α*$^{+/+}$*p53*$^{H/H}$ (black), *Hif1α*$^{+/-}$*p53*$^{H/H}$ (gray), *Hif1α*$^{KI/+}$*p53*$^{H/H}$ (white) mice. * $p < 0.05$, ** $p = 0.01$. B. Mitotic cells were identified by immunohistochemistry for phospho-histone H3 (Ser10). C. TUNEL staining of apoptotic cells. *Hif1α*$^{+/-}$ * $p = 0.01$, *Hif1α*$^{KI/+}$ $p = 0.14$ D. QRT-PCR analysis of HIFα and HIF target gene expression in thymic lymphomas from *Hif1α*$^{+/+}$*p53*$^{H/H}$, *Hif1α*$^{+/-}$*p53*$^{H/H}$, *Hif1α*$^{KI/+}$*p53*$^{H/H}$. * $p < 0.05$.

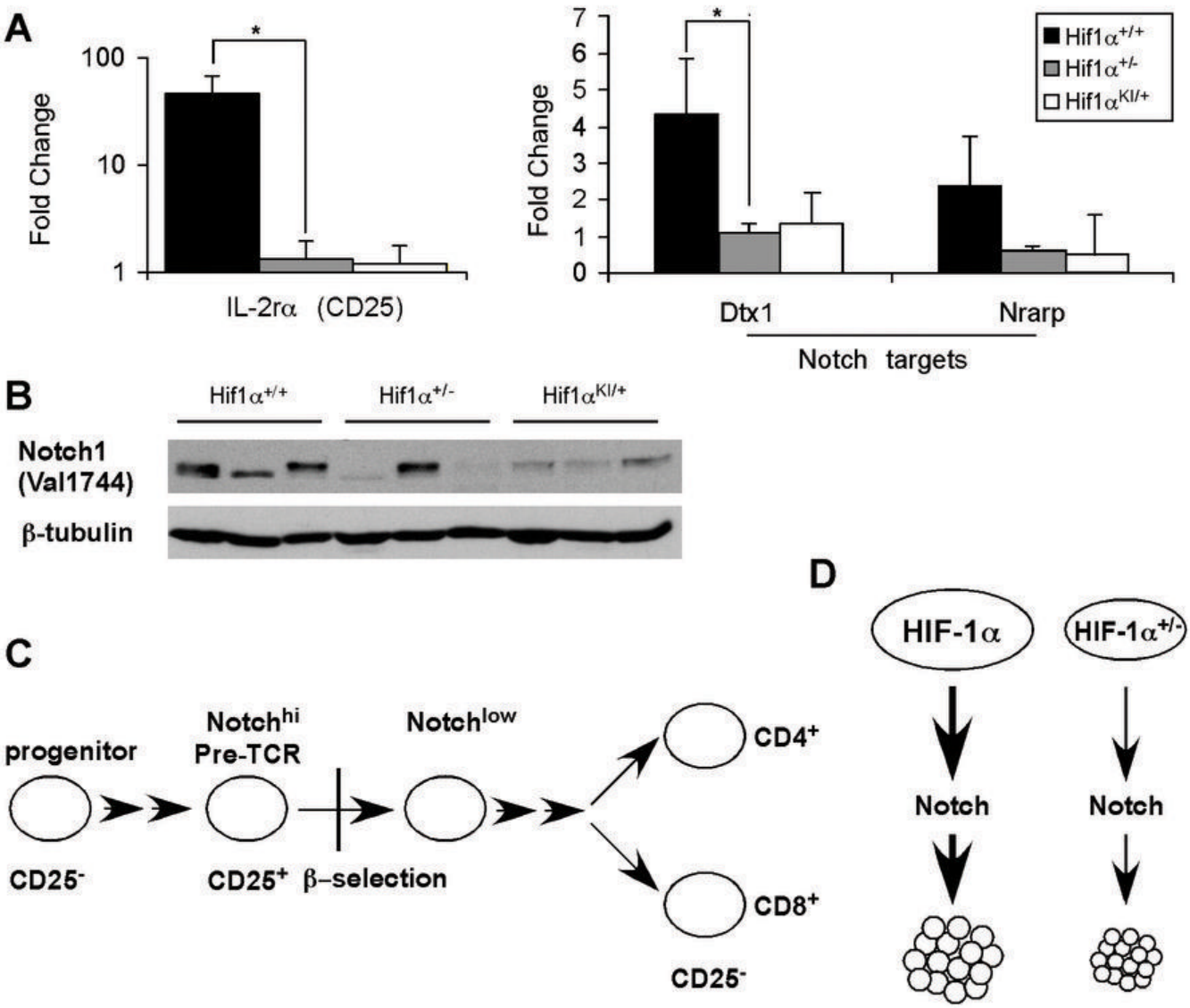

Figure 6. Differential activation of the Notch pathway in thymic lymphomas arising in *Hif1α*$^{+/+}$*p53*$^{H/H}$, *Hifα1*$^{+/-}$*p53*$^{H/H}$, and *Hif1α*$^{KI/+}$*p53*$^{H/H}$ mice

A. QRT-PCR for *IL-2 receptor-α* (CD25), *Dtx1* and *Nrarp*, two Notch target genes, in thymic lymphoma tissue derived from *Hif1α*$^{+/+}$*p53*$^{H/H}$ (n =9, black), *Hif1α*$^{+/-}$*p53*$^{H/H}$ (n = 7, gray), and *Hif1α*$^{KI/+}$*p53*$^{H/H}$ (n = 5, white) mice. * $p < 0.05$. B. Western blot for cleaved Notch (Val1744) using protein lysates derived from primary tumors. β–tubulin serves as the loading control. Differences in protein migration likely reflect changes in Notch1 phosphorylation. C. Model depicting the correlation between Notch activity and CD25 expression during T-cell development. D. Model depicting potential crosstalk between HIF1α levels and Notch activity in thymic lymphomas arising in *p53*$^{H/H}$ mice.